

Inelastic light scattering by collective charge-density excitations in semi-infinite semiconductor superlattices

Pawel Hawrylak, Ji-Wei Wu, and J. J. Quinn
Brown University, Providence, Rhode Island, 02912
(Received 10 May 1985)

An analytic expression for the resonant, inelastic light scattering cross section from collective charge-density excitations of a semi-infinite semiconductor superlattice is derived. Raman intensities of bulk and surface modes of an n -type GaAs-Al_xGa_{1-x}As sample are analyzed. Calculations show that intersubband surface plasmons have higher intensity than intrasubband ones and should be easier to observe experimentally. The line shapes of bulk spectra are explained in terms of photon broadening and broken translational symmetry in the superlattice direction. A new band of intersubband surface modes, with frequencies below the longitudinal-optical phonon frequency, is found.

I. INTRODUCTION

In the last few years resonant inelastic light scattering has been successfully applied to study single-particle and collective excitations of semiconductor superlattices.¹⁻⁴ While most experiments are performed with incident and scattered photons on the vacuum side of a semi-infinite superlattice, they are interpreted in terms of the bulk modes of infinite superlattices.^{5,6} The presence of an interface, however, is an essential ingredient of the problem. This has been demonstrated by recent theoretical study of collective charge-density excitations in such systems.⁷⁻⁹ A host of novel, intrasubband and intersubband surface modes has been predicted. These modes exist only for wavelengths shorter than a critical value λ^* , and they can be studied by inelastic light scattering. Raman intensities for light scattering from a semi-infinite array of two-dimensional electron-gas layers have been calculated recently by Jain and Allen.⁸ Katayama and Ando⁶ performed full self-consistent calculations of Raman intensities for an infinite superlattice in a multiple-quantum-well approximation. Clearly, the first approach does not take into account intersubband structure. The second fails to address the surface modes altogether, and required large numerical calculations. Here we adopt an intermediate approach. Using simple single-particle electronic states and various clearly stated approximations, we obtain an analytic expression for Raman intensities of intrasubband and intersubband excitations. This is used to predict conditions for observation of surface modes. The line shape of bulk spectrum is explained in terms of broken translational symmetry in the superlattice direction. Also, for a polar semiconductor superlattice, a new band of surface modes with frequencies below the longitudinal-optical frequency is found.

This article is organized as follows. In Sec. II we discuss inelastic light scattering from collective charge-density excitations via the three-step "carrier-density" mechanism. In Sec. III the integral equation for the polarizability of semi-infinite superlattice is solved, and in Sec. IV the Raman intensity is calculated analytically. This is used to calculate the dispersion of bulk and surface

collective modes of a selected n -type GaAs-Al_xGa_{1-x}As sample and to analyze their Raman spectra in Sec. V. Concluding remarks are contained in Sec. VI.

II. SCATTERING CROSS SECTION

Inelastic light scattering from charge-density excitations in semiconductors with arbitrary band structure has been discussed in detail by Jha,¹⁰ Blum,¹¹ Hamilton and McWhorter,¹² and others.¹³ Light scattering from two-dimensional plasmas has been considered qualitatively by Burstein, Pinczuk, and Mills.¹⁴ According to Burstein *et al.* the major contribution to the scattering cross section from collective excitations comes from a three-step carrier-density mechanism. In the first two steps an electron from the valence band in a given quantum well is optically excited to an empty state in any of the conduction-band subbands, and an electron from an occupied subband with identical spin annihilates the hole in the valence band. The net result is the excitation of an electron-hole pair which, via Coulomb interaction, generates collective excitations of the superlattice in a third step.

Following the formulation of Hamilton and McWhorter¹² and the recent work of Katayama and Ando,⁶ the differential cross section due to collective charge-density excitations per unit solid angle and per unit frequency interval may be written as

$$\frac{d^2\sigma}{d\omega_s d\Omega} = \frac{\omega_s}{\omega_i} \left[\frac{e^2}{mc^2} \right] |\hat{\epsilon}_i \cdot D \cdot D \hat{\epsilon}_s|^2 R^2(\omega_i) \times F(\omega_i - \omega_s, \mathbf{Q}^i - \mathbf{Q}^s), \tag{2.1}$$

where the function $F(\omega, \mathbf{Q})$ is given [$\mathbf{Q} = (\mathbf{q}, k_z)$] by

$$F(\omega, \mathbf{Q}) = \int_{-\infty}^{+\infty} dt e^{i\omega t} \int_{-\delta}^{\infty} \int_{-\delta}^{\infty} dz dz' \langle \rho^+(\mathbf{q}, z, t) \rho(\mathbf{q}, z', 0) \rangle \times \exp[i(k_z^i + k_z^s)z] \times \exp[-i(k_z^i + k_z^s)^* z']. \tag{2.2}$$

The resonant enhancement factor is given by¹²

$$R(\omega_i) = \frac{2|P_{VC}|^2}{3m} E_g / (E_g^2 - \omega_i^2). \quad (2.3)$$

Here P_{VC} is the valence-to-conduction-band momentum matrix element, evaluated at the bottom of the band, E_g is an appropriate gap energy ($E_0 + \Delta_0$ in most experiments), D is the transfer function connecting the fields inside and outside the sample,¹⁵ z is the axis of the superlattice (the vacuum-semiconductor interface is at $z = -\delta$), and $(\omega_i, \hat{\epsilon}_i, \mathbf{q}^i, k_z^i)$ and $(\omega_s, \hat{\epsilon}_s, \mathbf{q}^s, k_z^s)$ denote the frequency, polarization, and wave vectors of incident and scattered photons. Also, $\rho(\mathbf{x}, z, t)$ is the Fourier transform of the conduction-band density operator

$$\rho(\mathbf{q}, z, t) = \int d\mathbf{x} e^{-i\mathbf{q}\cdot\mathbf{x}} \rho(\mathbf{x}, z, t). \quad (2.4)$$

Formula (2.1) is valid for incident laser frequency ω_i close to the gap energy E_g , although $E_g - \omega_i$ is still large compared to typical intersubband energy difference.

With the use of fluctuation-dissipation theorem, the function $F(\omega, q)$ can be related to the imaginary part of the density-density correlation function $\Pi(\omega, q, z, z')$:

$$F(\omega, Q) = \frac{\hbar}{\Pi} [n(\omega) + 1] e^{-2\delta/\lambda} \int_{-\delta}^{\infty} \int_{-\delta}^{\infty} e^{-i2k(z-z')} \times e^{-(z+z')/\lambda} \text{Im}[-\Pi(\omega, q, z, z')] dz dz'. \quad (2.5)$$

Due to rotational symmetry in the plane perpendicular to the superlattice axis, functions F and Π depend only upon the magnitude of \mathbf{q} and $Q = (q, k)$. In Eq. (2.5) we have approximated k_z by⁸ $k_z = k + i/2\lambda$, where k and λ are defined by the equations

$$k = (\omega_i/c) \text{Re}\sqrt{\epsilon},$$

$$\frac{1}{\lambda} = 2(\omega_i/c) \text{Im}\sqrt{\epsilon}.$$

Thus $2k$ is the momentum transfer to the electronic excitation along the superlattice axis. ϵ is a background semiconductor dielectric constant and λ gives photon decay length inside the material. For GaAs, $\lambda \cong 6000$ Å, so that the effect of photon decay is negligible for single-particle excitations. However, for a superlattice this means that only 5–15 quantum wells close to the vacuum interface are strongly excited in the scattering experiment and the photon decay length cannot be neglected. This fact was first pointed out by Jain and Allen.⁸ To calculate the Raman intensity $F(Q, \omega)$ we need the density-density correlation function of the semiconductor superlattice.

III. DENSITY-DENSITY CORRELATION FUNCTION

The model system corresponding to the semiconductor superlattice under consideration is shown in Fig. 1. A semi-infinite array of quantum wells of thickness L , whose centers are separated by distance a occupies a half space $z > -\delta$, of background dielectric constant ϵ . An insulator with dielectric constant ϵ_0 occupies the space $z < -\delta$. We assume that single-particle electronic states are not changed by the presence of the interface from their bulk form and are given by

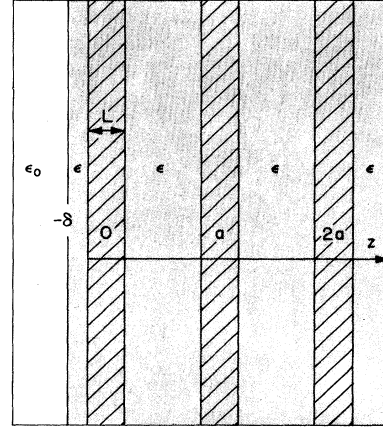


FIG. 1. Semi-infinite array of quantum wells (hatched area) of thickness L , whose centers are separated by distance a , embedded in a semiconductor with dielectric constant ϵ (shaded area). An insulator with dielectric constant ϵ_0 occupies the space to the left from the interface at $z = -\delta$.

$$|n, \mathbf{k}, l\rangle = e^{i\mathbf{k}\cdot\mathbf{r}} \xi_n(z - la). \quad (3.1)$$

Here n refers to subband index, \mathbf{k} is the momentum in the plane perpendicular to the z axis, and the interger l denotes the quantum well centered at $z = la$. We make the assumption that the wave functions $\xi_n(z)$ on different layers do not overlap, so that the minibands are flat.

The energy eigenvalues are

$$E_{nkl} = E_n + \frac{\hbar^2 k^2}{2m}, \quad (3.2)$$

where E_n is the energy at the bottom of each subband, and m is an effective mass.

The density-density correlation function $\Pi(\omega, q, z, z')$ has been discussed for infinite superlattice,⁶ layered electron gas,⁸ and inversion (accumulation) layers¹⁶ previously. It is sufficient to say that expanding density operators in terms of the real functions $\xi_n(z - la)$ allow us to write

$$\Pi(\omega, q, z, z') = \sum_{l, l'} \sum_{ijpt} \Pi_{ij,pt}(l, l') \xi_i(z - la) \xi_j(z - la) \times \xi_p(z' - l'a) \xi_t(z' - l'a). \quad (3.3)$$

Within the random-phase approximation (RPA), $\Pi_{ij,pt}(l, l')$ satisfy an integral equation

$$\Pi_{ij,pt}(l, l') = \Pi_{ij}^0 \delta_{it} \delta_{jp} \delta_{l, l'} + \sum_{r, s, l''} \Pi_{ij}^0 V_{ij,rs}(l, l'') \times \Pi_{rs,pt}(l'', l'). \quad (3.4)$$

Π_{ij}^0 , the polarizability of the noninteracting system, is layer independent and given by

$$\Pi_{ij}^0(q, \omega) = 2 \sum_{\mathbf{k}} \frac{f(\epsilon_{j, \mathbf{k}+\mathbf{q}}) - f(\epsilon_{i, \mathbf{k}})}{\epsilon_{j, \mathbf{k}+\mathbf{q}} - \epsilon_{i, \mathbf{k}} - \hbar\omega}. \quad (3.5)$$

The electron-electron interaction is given by

$$V_{ij,rs}(l,l') = V_q \int \int dz dz' \xi_i(z-la) \xi_j(z-la) \\ \times (e^{-q|z-z'|} + \alpha e^{-q(z+z')}) \\ \times \xi_r(z'-l'a) \xi_s(z'-l'a). \quad (3.6)$$

The terms within parentheses are Fourier transforms of direct and image Coulomb interactions, respectively. Also, V_q and α are given by

$$V_q = 2\Pi e^2 / \epsilon(\omega) q, \quad (3.7)$$

$$\alpha = e^{-2\delta q} \frac{\epsilon(\omega) - \epsilon_0}{\epsilon(\omega) + \epsilon_0}, \quad (3.8)$$

so that interaction with optical phonons can be taken into account via the frequency-dependent dielectric function $\epsilon(\omega)$.

In solving Eq. (3.4) we limit ourselves to the case of zero temperature and low electron densities so that only lowest subband is occupied. Furthermore, we employ the commonly used diagonal approximation,¹⁶ which decouples different intersubband excitations. Equation (3.4) can then be written in a simple form for every $0 \rightarrow m$ subband transition

$$\chi_m(l,l') = \chi_m^0 \delta_{l,l'} + \chi_m^0 \sum_{l''} V_{m,m}(l,l'') \chi_m(l'',l'), \quad (3.9)$$

where $\chi_m^0 = \Pi_{0m} + \Pi_{m0}$ for $m \neq 0$ and $\chi_0^0 = \Pi_{00}$, and $V_{m,m}(l,l') = V_{m0,0m}(l,l')$. Formal solution to Eq. (3.9) can be obtained by defining a dielectric matrix $\epsilon(l,l';m)$

$$\epsilon(l,l';m) = \delta_{l,l'} - \chi_m^0 V_{m,m}(l,l') \quad (3.10)$$

and its inverse as $\epsilon^{-1}(l,l';m)$. Now the polarizability matrix $\chi_m(l,l')$ can be written in a familiar way,

$$\chi_m(l,l') = \chi_m^0 \epsilon^{-1}(l,l';m). \quad (3.11)$$

Using Eqs. (3.3) and (3.11), we can finally write the density-density correlation function as

$$\Pi(\omega, q, z, z') = \sum_{m=0,1,\dots} \sum_{l,l'} \chi_m^0 \epsilon^{-1}(l,l';m) \psi_m(z-la) \\ \times \psi_m(z'-l'a), \quad (3.12)$$

where $\psi_m(z-la) = \xi_m(z-la) \xi_0(z-la)$.

Note that dielectric matrix $\xi(l,l';m)$ given by Eq. (3.10) has been derived by us earlier using self-consistent linear-density-response theory.⁹ Zeros of $\epsilon(l,l';m)$ yield in a very simple way surface and bulk collective modes, the later in complete agreement with the theory of Tselis and Quinn.¹⁷ However, here we need an inverse of the dielectric matrix. In order to find $\epsilon^{-1}(l,l';m)$ [or solve Eq. (3.9)] we make use of the transformation introduced re-

cently by Jain and Allen⁸ for a semi-infinite array of electron-gas layers. Since they discussed this transformation in detail, only a brief sketch will be given in the Appendix. Here we give the final result:

$$\epsilon^{-1}(l,l';m) = \delta_{l,l'} \gamma^{-1} + \frac{\chi_m^0 V_q G_{-m} \sinh(qa) e^{-\beta|l-l'|}}{\gamma^2 (b^2 - 1)^{1/2}} \\ + \frac{\chi_m^0 V_q (e^{2\beta} A - 2B e^\beta + C) e^{-\beta(l+l')}}{\gamma^2 2e^{2\beta} (b^2 - 1) Q}. \quad (3.13)$$

Here all quantities are defined as follows:

$$\gamma = 1 - \chi_m^0 V_q (V_{-m} - G_{-m}), \quad (3.14)$$

$$b = \cosh(qa) - \chi_m^0 V_q G_{-m} \sinh(qa) / \gamma, \quad (3.15)$$

$$e^\beta = b + (b^2 - 1)^{1/2}, \quad (3.16)$$

$$a_0 = G_{-m} + \frac{\alpha}{2} e^{qa} G_{+m}, \quad (3.17)$$

$$b_0 = G_{-m} \cosh(qa) + \frac{\alpha}{2} e^{qa} G_{+m}, \quad (3.18)$$

$$c_0 = G_{-m} + \frac{\alpha}{2} G_{+m}, \quad (3.19)$$

$$H = \frac{1}{2} \frac{e^{-\beta(b^2 - 1)^{-1/2}} - e^{-qa} \sinh(qa)^{-1}}{[\sinh(qa) G_{-m}]}, \quad (3.20)$$

$$G = \frac{1}{2} [(b^2 - 1)^{-1/2} - \sinh(qa)^{-1}] / [\sinh(qa) G_{-m}], \quad (3.21)$$

$$Q = 1 - G(a_0 + c_0) + 2b_0 H + (H^2 - G^2)(b_0^2 - a_0 c_0), \quad (3.22)$$

$$A = G(b_0^2 - a_0 c_0) + a_0, \quad (3.23)$$

$$B = H(b_0^2 - a_0 c_0) + b_0, \quad (3.24)$$

$$C = G(b_0^2 - a_0 c_0) + c_0, \quad (3.25)$$

$$V_{\pm m} = \int \int dz dz' \psi_m(z)^{-q|z \pm z'|} \psi_m(z'). \quad (3.26)$$

The matrix elements $G_{\pm m}(q)$ are defined by a similar expression, except for the replacement of $|z \pm z'|$ by $(z \pm z')$. Here e^β is defined such that $|e^\beta| > 1$. If not, the replacement $(b^2 - 1)^{1/2}$ by $-(b^2 - 1)^{1/2}$ is understood in Eqs. (3.14)–(3.26).

The first two terms in Eq. (3.13) give the bulk contribution, while the last term which decays away from the surface, gives the surface correction. Equation (3.13) reduces exactly to the result of Jain and Allen if we set $m=0$, $V_{\pm m} = G_{\pm m} = \gamma = 1$ as appropriate for layered electron gas.

IV. RAMAN INTENSITIES

The Raman intensity is proportional to the function $F(\omega, Q)$. Using Eqs. (2.4) and (3.12), we have (at $T=0$)

$$F(\omega, Q) = \sum_m \sum_{l,l'} e^{-2\delta/\lambda} \int_{-\delta}^{\infty} \int_{-\delta}^{\infty} dz dz' \text{Im}[-\chi_m^0 \epsilon^{-1}(l,l';m)] e^{-2ik(z-z')} e^{-(z+z')/\lambda} \psi_m(z-la) \psi_m(z'-l'a). \quad (4.1)$$

Noting that $\exp[-i2k(z-z')]$ under the double integral and double sum over l , and l' is real, we can carry all

operations in Eq. (4.1) with $\chi_m^0 \epsilon^{-1}(l,l';m)$ and take the imaginary part at the end:

$$F(\omega, Q) = \sum_m \text{Im} \left[- \sum_{l, l'} A_m \chi_m^0 \epsilon^{-1}(l, l'; m) e^{-i2k(l-l')a} \times e^{-(l+l')a/\lambda} \right] \quad (4.2)$$

with an amplitude A_m given by

$$A_m = e^{-2\delta/\lambda} \int \int dz dz' e^{-2ik(z-z')} e^{-(z+z')/\lambda} \times \psi_m(z) \psi_m(z'). \quad (4.3)$$

Now all sums may be done explicitly, and we have the final expression for $F(\omega, Q)$,

$$F(\omega, Q) = \sum_m A_m \text{Im} \left[-\chi_m^0 \frac{1}{\epsilon_m(\omega, q, 2k)} \right], \quad (4.4)$$

where the effective inverse dielectric function $1/\epsilon_m$ is given by

$$\frac{1}{\epsilon_m(\omega, q, 2k)} = \frac{\gamma^{-1}}{1 - e^{-2a/\lambda}} + \frac{\chi_m^0 V_q G_{-m} \sinh(qa) (e^{2\beta} e^{2a/\lambda} - 1)}{(1 - e^{-2a/\lambda})^2 (b^2 - 1)^{1/2} E} + \frac{\chi_m^0 V_q (e^{2\beta} A - 2B e^\beta + C)}{2E(b^2 - 1)Q} e^{2a/\lambda} \quad (4.5)$$

and

$$E = 1 + e^{2\beta + 2a/\lambda} - 2e^{\beta + a/\lambda} \cos(2ka). \quad (4.6)$$

Equations (4.4)–(4.6) are the main result of this work. We have obtained an analytic expression for the Raman intensity as the sum of contributions from all intrasubband and intersubband collective excitations, as indicated by the presence of the effective inverse dielectric function. Each contribution is weighted by an amplitude A_m which, without photon decay, is simply a square of the usual matrix element by which light couples to charge density, i.e.,

$$A_m = |\langle 0 | e^{2ikz} | m \rangle|^2.$$

Note that as in Eq. (3.13), $1/\epsilon$ consists of bulk (first two terms) and surface parts. Bulk collective modes are given by the solution to $E(\lambda \rightarrow \infty) = 0$ and surfaced modes by the solution to $Q(q, \omega) = 0$. As expected, broadening due to the decay of the photon inside the semiconductor affects only bulk excitations. In the next paragraph an example of Raman intensities is given.

V. RESULTS

Here we predict Raman intensities $F(\omega, Q)$ for an n -type GaAs-Al_xGa_{1-x}As sample, studied experimentally by Pinczuk *et al.*,¹ and theoretically by Katayama *et al.*,⁶ in backscattering geometry. This sample has only the lowest subband occupied; therefore, our calculations are applicable. Note that currently available experimental spectra for finite in-plane wave-vector transfer were obtained from samples with several subbands filled. The parameters for this sample are $L=200$ Å, $a=404$ Å, the electron density $n=4.2 \times 10^{11}$ cm⁻², and the effective

mass $m=0.068m_e$. We use GaAs background dielectric constant

$$\epsilon(\omega) = \epsilon_\infty \frac{\omega^2 - \omega_{\text{LO}}^2 + i\gamma_{\text{ph}}\omega}{\omega^2 - \omega_{\text{TO}}^2 + i\gamma_{\text{ph}}\omega} \quad (5.1)$$

with longitudinal-optical (LO) and transverse-optical (TO) phonon frequencies of $\hbar\omega_{\text{LO}}=36.7$ meV, $\hbar\omega_{\text{TO}}=33.6$ meV. $\epsilon_\infty=11.1$ and γ_{ph} is the phenomenological width. For simplicity, long-wavelength forms of $\chi_m^0(q, \omega)$ have been taken, i.e.,

$$\chi_0^0 = \frac{nq^2}{m(\omega^2 + i\gamma_e\omega)}, \quad \chi_m^0 = \frac{2nE_{m0}}{\omega^2 - E_{m0}^2 + i\gamma_e\omega}$$

with γ_e being the phenomenological broadening, related to mobility in the usual way. A single-particle energy separation of $E_{10}=21.7$ meV has been taken from experiment⁵ and all matrix elements $V_{\pm m}, G_{\pm m}, A_m$ have been approximated by those of infinite wells.⁹ Should an experimental data become available, calculations can be easily refined.¹⁸

First we turn our attention to the dispersion of bulk and surface collective modes. They are given by the equations $E(\omega, q, k)=0$ and $Q(\omega, q)=0$ for bulk and surface modes.

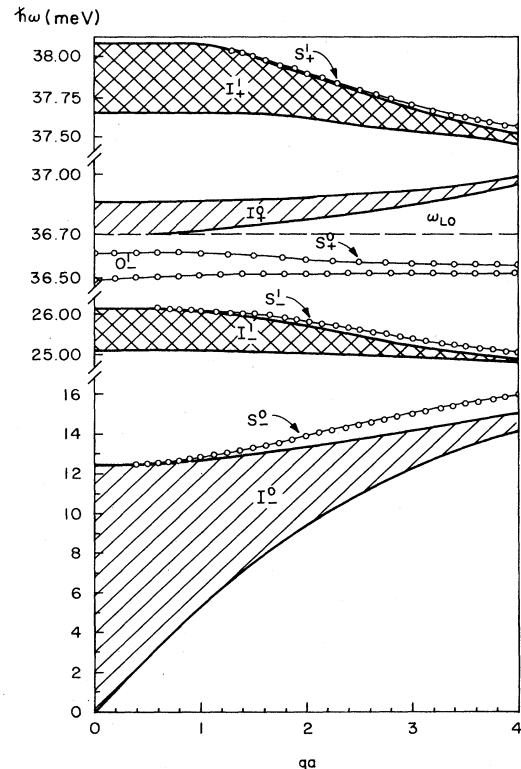


FIG. 2. Dispersion relation ω vs q for bulk (shaded area) and surface (dashed line) intrasubband ($m=0$) and intersubband ($m=1$) modes. The values of parameters are as follows: $n=4.2 \times 10^{11}$ cm⁻², $a=404$ Å, $L=200$ Å, $2\delta=L$, $m=0.068m_e$, $\epsilon_\infty=11.1$, $\hbar\omega_{\text{LO}}=36.7$ meV, $\hbar\omega_{\text{TO}}=33.6$ meV, $E_{10}=21.7$ meV. Bulk (surface) modes are denoted by $I_{+,-}^m$ ($S_{+,-}^m$); O^m are new surface modes associated with intersubband transitions. For better visibility different energy scales are used.

These equations are completely equivalent to the ones derived by us from the zeros of the dielectric matrix; for the bulk modes they reproduce the results of Tselis and Quinn.¹⁷ The results are shown in Fig. 2 for $m=0$ (intrasubband modes) and $m=1$ (lowest intersubband modes). Due to mixing with LO phonons we have two coupled electron-phonon bands for each transition which we denote by $I_{+,-}^m$, where $+$ ($-$) stands for higher (lower) energy mode for $0-m$ transition. Intrasubband and intersubband surface modes are denoted by $S_{+,-}^m$. Surface modes exist because of the difference of dielectric constants between an insulator and semiconductor. There are two modes associated with intrasubband transitions, a surface plasmon S_-^0 which exists only for wave vectors larger than $qa=0.4$ and a surface phononlike mode S_+^0 which exists for arbitrary wave vector and has a frequency below ω_{LO} . Two surface wave modes associated with intersubband excitations exist for the wave vectors larger than $qa=0.6$ and $qa=1.3$ for S_-^1 and S_+^1 , respectively. Note, however, that there is an extra mode with frequency below ω_{LO} associated with $0-1$ intersubband transition. In fact, there should be a band of modes below ω_{LO} , one mode for each intersubband excitation. This is a new feature not reported previously, a superlattice analog of the trapped surface modes in accumulation layers recently discovered by Puri and Schaich.¹⁹

We now turn to Raman intensities $F(\omega, Q)$ as given by Eq. (4.4) for the following parameters:²⁰ $qa=1$, $ka=2.828$, and $\gamma_e=\gamma_{ph}=0.1$ meV. An overall spectrum is shown in Fig. 3. The dominant feature is the peak due to bulk intersubband transitions I_-^1 with a much weaker peak due to I_+^1 and intersubband plasmon I_-^0 . Surface plasmons are also indicated. Clearly the intersubband plasmon S_-^1 has the highest intensity and would be easiest to detect experimentally. In Fig. 4 an intrasubband spectrum is shown. The peak at 10.9 meV is due to bulk plasmon and at 12.86 meV is due to the surface plasmon. The broadening of the former is due to photon decay while that of the latter is controlled by γ_e . Since intrasubband plasmons are often approximated by plasmons of an array of two-dimensional layers,^{7,8} it is interesting to compare the two spectra. As we can see from Fig. 4, qualita-

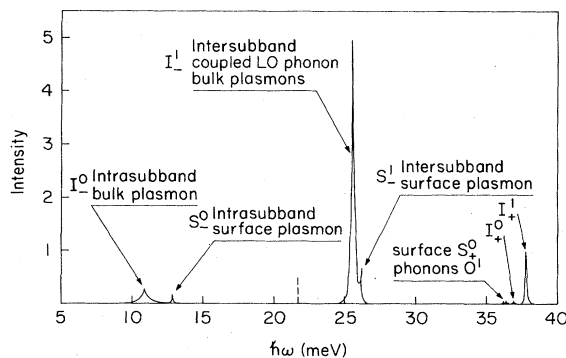


FIG. 3. Raman intensities for bulk and surface plasmons for in-plane momentum transfer $qa=1$, and for momentum transfer along the superlattice axis of $2ka=5.656$ ($m=0,1$ only). And $\gamma_e=\gamma_{ph}=0.1$ meV.

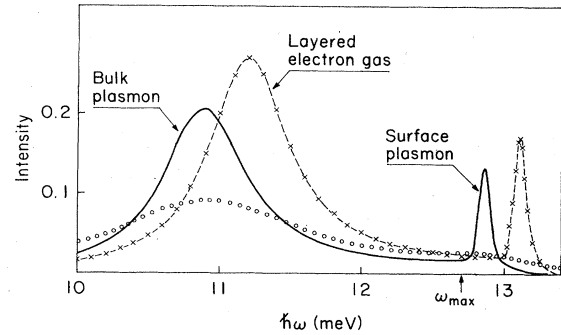


FIG. 4. Raman intensity for intrasubband bulk and surface plasmon for parameters as in Fig. 3. For comparison, Raman intensity from layered electron gas is shown (dashed line).

tive agreement is quite good but there is clearly a quantitative difference both in overall intensity and position of the resonances.

In Figs. 5 and 6 Raman intensities for the intersubband excitations are shown in detail. Here we plot bulk and surface contributions to the total intensity. The cancellation between bulk and surface contributions, both of which display sharp structure at the boundary of the bulk plasmon band, is illustrated. This remarkable feature has been pointed out by Jain and Allen⁸ for an array of electron-gas layers. They attributed the singular behavior in the bulk part to the divergence of the density of states of a one-dimensional plasmon band at the band edge (Van Hove singularity). The surface part cancels this divergence, but this has not yet been explained. It can be understood if we realize that the bulk part is the answer one would obtain for a translationally invariant system, i.e., such that the Hamiltonian $V(z,z')=V(z-z')$ and the

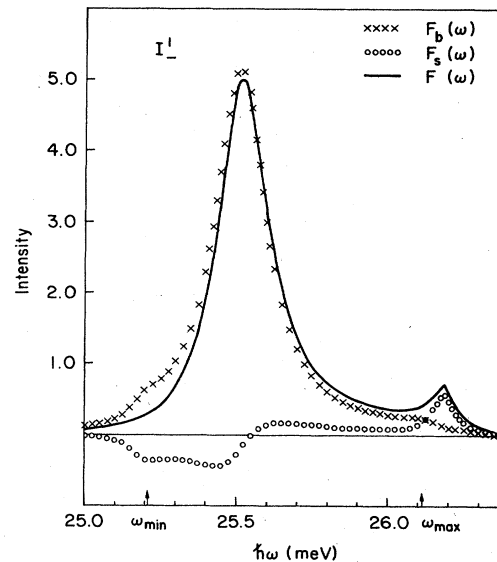


FIG. 5. Raman intensity from intersubband bulk I_-^1 and surface S_-^1 plasmons. Here contributions from surface and bulk parts are shown. Band boundaries are indicated by ω_{min} and ω_{max} . (All parameters as in Figs. 3 and 4.) Surface plasmon is visible above the upper band edge.

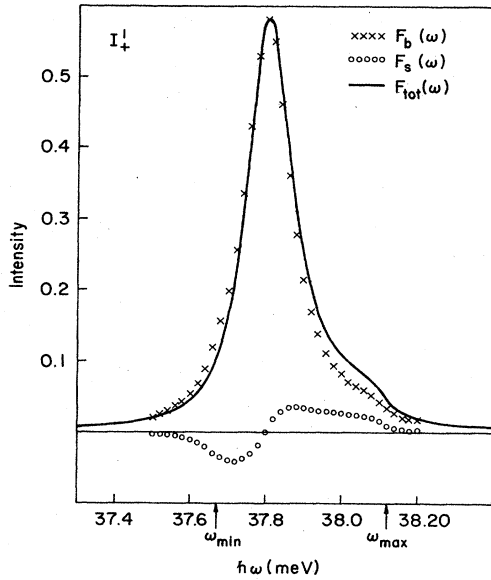


FIG. 6. Raman intensity from intersubband bulk plasmon I_+^1 . Note asymmetric broadening due to a surface plasmon "emerging" in a continuous way from the bulk band. (All parameters as in Figs. 3–5.)

periodic boundary conditions can be applied. Due to the interface, translational symmetry of the system is broken. Hence two necessary conditions for the existence of Van Hove singularities are not met. Since matrix $\epsilon(l, l'; m)$ is *exactly* inverted (see the Appendix for more details), full answer to the intensity does not show any structure at the band edge.

The surface intersubband plasmon S_-^1 , shown in Fig. 5, is significantly broadened due to its closeness to the bulk plasmon band. While the dispersion relation predicts no S_+^1 plasmon at this wave vector, we see clearly a shoulder on the high-energy side of the I_+^1 peak (Fig. 6). This asymmetric broadening is due to the surface plasmon which emerges from the bulk spectrum in a continuous way when broadening due to finite mobility is included.

The Raman intensity of the surface modes with energies below ω_{LO} is shown in Fig. 7. Their intensity is very weak, with the intensity of the intersubband mode higher than that of the intrasubband mode.

VI. CONCLUSIONS

In summary, an analytic expression for the cross section of the inelastic light scattering from collective charge-density excitations of a semi-infinite semiconductor or superlattice has been derived. Basic approximations involve simple single-particle electronic states and decoupling of intersubband excitations. The results are valid for low-density samples, i.e., those with only the lowest subband occupied.

We have analyzed Raman intensities of bulk and surface collective modes of an existing n -type GaAs- $\text{Al}_x\text{Ga}_{1-x}\text{As}$ sample for realistic values of parameters. Bulk spectra reveal broken translational symmetry in the superlattice direction, manifested by the lack of structure

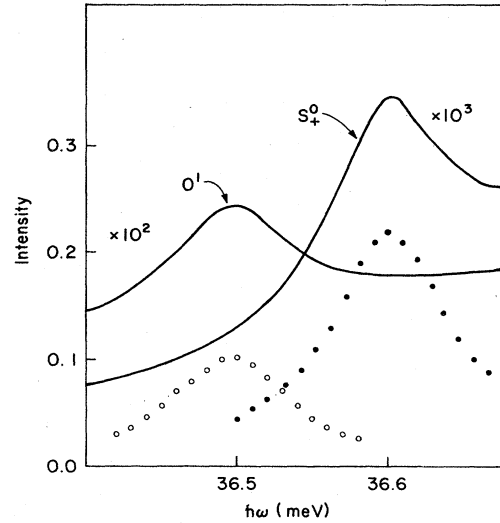


FIG. 7. Raman intensities from surface modes with frequencies below ω_{LO} . Surface contribution is shown by a dotted line. (All parameters as in Figs. 3–6.)

at the plasmon band edges. Our results suggest that while intrasubband collective surface modes have received most of the attention up to now, it is the intersubband surface modes which should be more easily observed in experiment. New surface modes, with energies below ω_{LO} , couple to light very weakly and should be difficult to observe. We feel that our results, although only semiquantitative, should prove very useful in interpreting experimental results.

ACKNOWLEDGMENTS

The authors would like to thank Professor J. K. Jain, Professor P. B. Allen, Professor S. Katayama, and Professor T. Ando for providing results of their work prior to publication. Financial support of the U.S. Army Research Office, Durham, is acknowledged.

APPENDIX

Here we outline the solution to Eq. (3.9), i.e., the way the inverse dielectric matrix is computed. Equation (3.9) reads

$$\chi_m^0(l, l') = \chi_m^0 \delta_{l, l'} + \sum_{l''=0}^{N-1} \chi_m^0 V_q V_{m, m}(l, l'') \chi_m(l'', l'). \quad (\text{A1})$$

Matrix elements $V_{m, m}(l, l')$ can be written, after simple algebra, from Eq. (3.6) (we omit subscript m and q, ω dependence of all quantities) as

$$V(l, l') = (V_{-m} - G_{-m}) \delta_{l, l'} + G_{-m} e^{-q|l-l'|a} + \alpha G_{+m} e^{-q(l+l')a}. \quad (\text{A2})$$

Symbols V_q , α , $V_{\pm m}$, and $G_{\pm m}$ have been defined in the text [Eqs. (3.7), (3.8), and (3.26)]. Note that Eq. (A1) is written for a finite system of N quantum wells, and its solution has now been reduced to an N -layer problem. The layers are labeled by index l ($l=0, 1, \dots, N-1$).

The first ($l=0$) and last ($l=N-1$) layers are not equivalent due to the interface with vacuum at $l=0$. Hence no mirror symmetry can be assumed; yet all quantities can be expanded in the basis of orthogonal functions on $(0, N-1)$, e.g.,

$$\chi(k, k') = \frac{1}{N} \sum_{l, l'} e^{-ikla} \chi(l, l') e^{ik'l'a} \quad (\text{A3})$$

and inverse transform

$$\chi(l, l') = \frac{1}{N} \sum_{k, k'} e^{ikla} \chi(k, k') e^{-ik'l'a}, \quad (\text{A4})$$

where

$$k = \frac{2\pi}{a} \frac{n}{N}, \quad n = 0, 1, 2, \dots, N-1.$$

This transformation was used recently by Jain and Allen.⁸ Fourier transform of Eq. (A1) gives

$$\chi(k, k') = \chi^0 \delta_{k, k'} + \chi^0 V_q \sum_{k''} V(k, k'') \chi(k'', k). \quad (\text{A5})$$

We write $V(k, k')$ in terms of "bulk" and "surface" parts where bulk part merely means a part diagonal in k space and surface part is the rest:

$$V(k, k') = V^b(k) \delta_{k, k'} + V^s(k, k'), \quad (\text{A6})$$

where (q, k measured in units of a)

$$V^b(k) = V_- - G_- + G_- S(k), \quad (\text{A7})$$

$$V^s(k, k') = \frac{1 - e^{-qN}}{2NP(k)P(k')} [a_0 - b_0(e^{ik} + e^{-ik'}) + c_0 e^{i(k-k')}], \quad (\text{A8})$$

$$P(k) = \cosh(q) - \cos(k), \quad (\text{A9})$$

$$S(k) = \sinh(q)/P(k), \quad (\text{A10})$$

and a_0, b_0, c_0 , are given by Eqs. (3.17)–(3.19). In analogy to Eq. (A6) we split $\chi(k, k')$ into the diagonal (bulk) part and the rest

$$\chi(k, k') = \chi^b(k) \delta_{k, k'} + \chi^s(k, k'). \quad (\text{A11})$$

Substitution of Eqs. (A11) and (A6) into Eq. (A5) gives two coupled equations; for the bulk part (diagonal) and the rest (surface part):

$$\chi^b(k) \delta_{k, k'} = \chi^0 \delta_{k, k'} + \chi^0 V_q V^b(k) \chi^b(k) \delta_{k, k'}, \quad (\text{A12})$$

$$\begin{aligned} \chi^s(k, k') &= \chi^0 V_q V^b(k) \chi^s(k, k') + \chi^0 V^s(k, k') \chi^b(k') \\ &+ \chi^0 V_q \sum_{k''} V^s(k, k'') \chi^s(k'', k'). \end{aligned} \quad (\text{A13})$$

Equation (A12) can easily be solved, giving the bulk part of the susceptibility:

$$\chi^b(k) = \frac{\chi^0 \delta_{k, k'}}{1 - \chi^0 V_q V^b(k)} = \frac{\chi^0}{\epsilon(k)} \delta_{k, k'}. \quad (\text{A14})$$

This is precisely the answer one obtains for a *translationally invariant system*, hence the name bulk. Using (A14) we can write Eq. (A13) for the surface (off-diagonal) part of the polarizability:

$$\begin{aligned} \chi^s(k, k') &= \frac{(\chi^0)^2 V_q}{\epsilon(k)\epsilon(k')} V^s(k, k') \\ &+ \frac{\chi^0 V_q}{\epsilon(k)} \sum_{k''} V^s(k, k'') \chi^s(k'', k'). \end{aligned} \quad (\text{A15})$$

Examination of the structure in k space of the bare vertex $V^s(k, k')$ allows us to write the solution to Eq. (A15) in the form

$$\chi^s(k, k') = \frac{1 - e^{-qN}}{2N} \chi_0^2 V_q \frac{A - B(e^{ik} + e^{-ik'}) + C e^{i(k-k')}}{P(k)\epsilon(k)P(k')\epsilon(k')}. \quad (\text{A16})$$

Substitution of (A16) to (A15) yields three equations for coefficients A, B, C , whose solution (in the large- N limit) is given in Sec. III. From Eq. (A16) we see that the surface contribution is proportional to $1/N$, while the bulk part [Eq. (A14)] is not. However, if the surface part is neglected, the inverse transform is violated and the important part of $\chi(l, l')$ is lost.

Note that at no place was it essential that the potential $V(l, l')$ be of the form $V(l-l')$. For any finite N translational symmetry of the system is broken. But the density of states of a finite system does not diverge (no Van Hove singularities), even though its normal modes can still be characterized by a quantum number k_z . Hence there should be no divergence in Raman intensities at the plasmon band edges if the full, *exact* solution is used. Also, there must be no contribution from the surface part at the resonance since normal modes of a finite system and infinite one (but periodic) are identical. This is seen in Figs. 5 and 6. It is the ability to solve *exactly* Eq. (A1) which reveals broken translational symmetry in the Raman intensities.

Note that translational symmetry and periodic boundary conditions are merely a clever method we use to solve problems which would otherwise be intractable. Here we have a finite system (30–100 layers) and an exact solution is possible.

¹A. Pinczuk, J. M. Worlock, H. L. Stormer, R. Dingle, W. Wiegmann, and A. C. Gossard, *Solid State Commun.* **36**, 43 (1980).

²D. Olego, A. Pinczuk, A. C. Gossard, and W. Wiegmann, *Phys. Rev. B* **25**, 7867 (1982).

³R. Sooryakumar, A. Pinczuk, A. Gossard, and W. Wiegmann, *Phys. Rev. B* **31**, 2578 (1985).

⁴Ch. Zeller, G. Abstreiter, and K. Ploog, *Surf. Sci.* **113**, 85 (1982).

⁵A. Pinczuk and J. M. Worlock, *Surf. Sci.* **113**, 69 (1982).

⁶S. Katayama and T. Ando, *J. Phys. Soc. Jpn.* **54**, 1615 (1985).

⁷G. F. Giuliani and J. J. Quinn, *Phys. Rev. Lett.* **51**, 919 (1983).

⁸J. K. Jain and P. B. Allen, *Phys. Rev. Lett.* **54**, 947 (1984); *Phys. Rev. B* **32**, 997 (1985).

- ⁹P. Hawrylak, J.-W. Wu, and J. Quinn, Phys. Rev. B (to be published).
- ¹⁰S. S. Jha, Nuovo Cimento B **63**, 331 (1969).
- ¹¹F. Blum, Phys. Rev. B **1**, 1125 (1970).
- ¹²D. C. Hamilton and A. L. McWhorter, *International Conference on Light Scattering of Solids, 1968*, edited by G. B. Wright (Springer, New York, 1969), p. 309.
- ¹³For a review, see M. V. Klein, in *Light Scattering in Solids*, edited by M. Cardona (Springer, New York, 1975), p. 147.
- ¹⁴E. Burstein, A. Pinczuk, and D. L. Mills, Surf. Sci. **98**, 451 (1980).
- ¹⁵S. Katayama and K. Murase, J. Phys. Soc. Jpn. **42**, 886 (1977).
- ¹⁶G. H. Kawamoto, J. J. Quinn, and W. L. Bloss, Phys. Rev. B **23**, 1875 (1981); D. L. Dahl and L. J. Sham, *ibid.* **16**, 651 (1977).
- ¹⁷A. C. Tselis and J. J. Quinn, Phys. Rev. B **29**, 3318 (1984).
- ¹⁸G. Fishman, Phys. Rev. B **27**, 7611 (1983).
- ¹⁹A. Puri and W. L. Schaich, Phys. Rev. B **31**, 974 (1985).
- ²⁰The choice of the $2ka$ in our numerical example corresponds to the energy $2(E_g + \Delta_0)$ of GaAs, i.e., is off the resonant enhancement. For energies close to E_g we find a very weak intensity of the surface intrasubband plasmon and higher intensity for the intersubband plasmon but poorly resolved from the bulk spectrum.

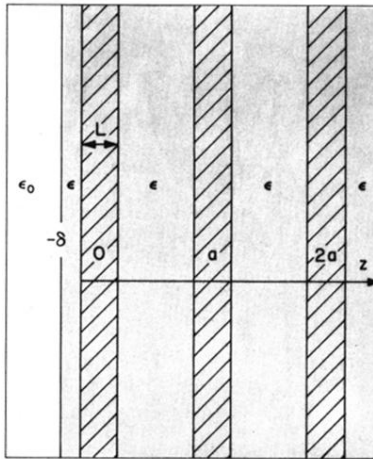


FIG. 1. Semi-infinite array of quantum wells (hatched area) of thickness L , whose centers are separated by distance a , embedded in a semiconductor with dielectric constant ϵ (shaded area). An insulator with dielectric constant ϵ_0 occupies the space to the left from the interface at $z = -\delta$.